Electronic Supplementary Material (ESI) for Lab on a Chip.

Supplementary Information

Prediction of tumor metastasis via extracellular vesicles-treated platelet adhesion on a blood vessel chip

Junyoung Kim[a,b], Vijaya Sunkara[a], Jungmin Kim[a,b], Jooyoung Ro[a,b], Chi-Ju Kim[a], Elizabeth Maria Clarissa[b], Sung Wook Jung[c], Hee Jin Lee[c], Yoon-Kyoung Cho[a,b*]

[a.] Center for Soft and Living Matter, Institute for Basic Science (IBS), Ulsan 44919, Republic of Korea

[b.] Department of Biomedical Engineering, School of Life Sciences, Ulsan National Institute of Science and Technology (UNIST), Ulsan 44919, Republic of Korea

[c.] Department of Pathology, Asan Medical Center, University of Ulsan College of Medicine, Seoul, 05505, Republic of Korea

* E-mail: ykcho@unist.ac.kr

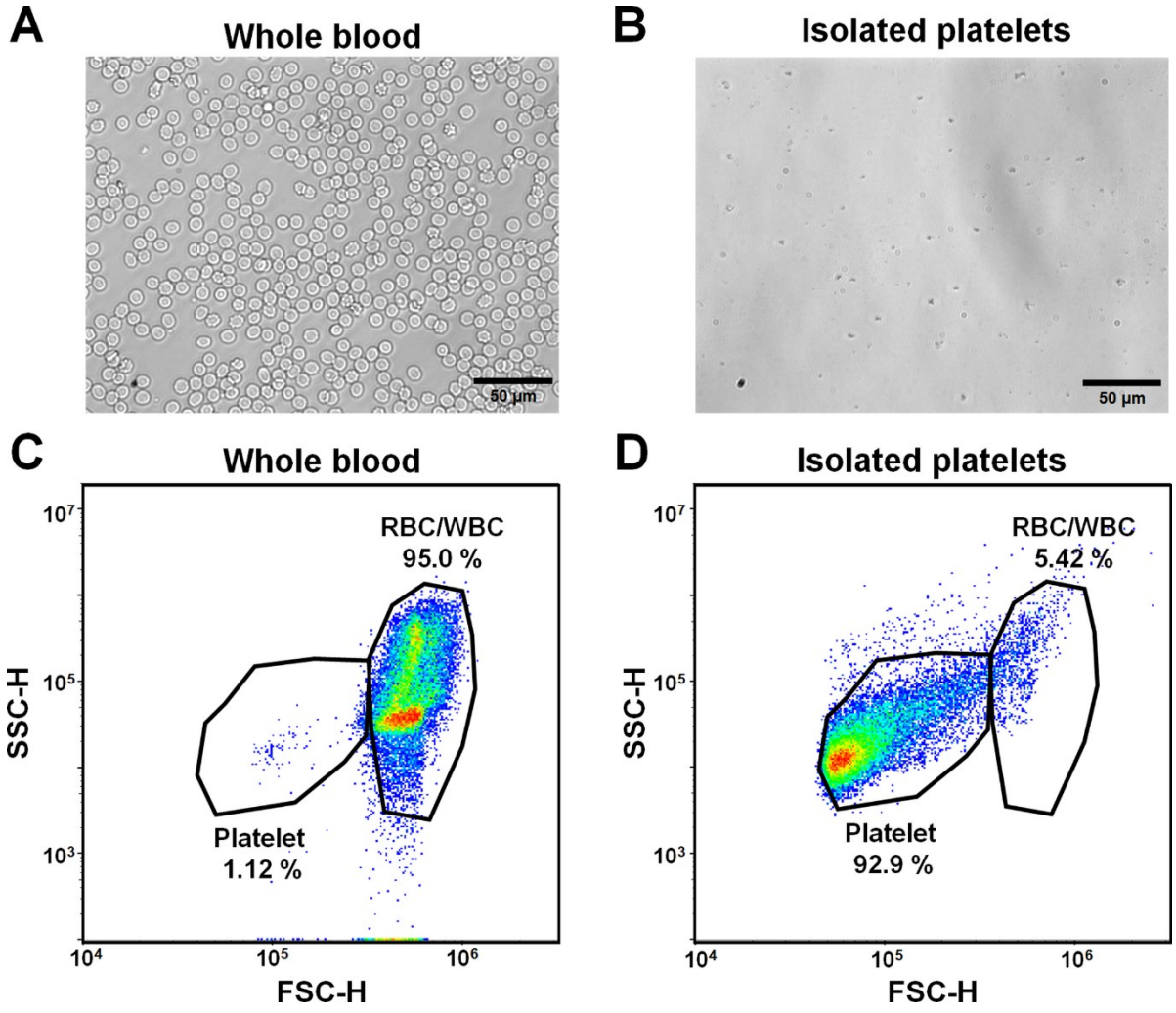

Figure S1. Separation of platelets from whole blood. (A-B) Microscopic images of whole blood and purified platelets. **(C-D)** Flow cytometric analysis of whole blood and purified platelets. In whole blood, there are red blood cells (RBCs), white blood cells (WBCs), and platelet populations. After the separation of platelets from whole blood, RBC and WBC populations were observed to reduce.

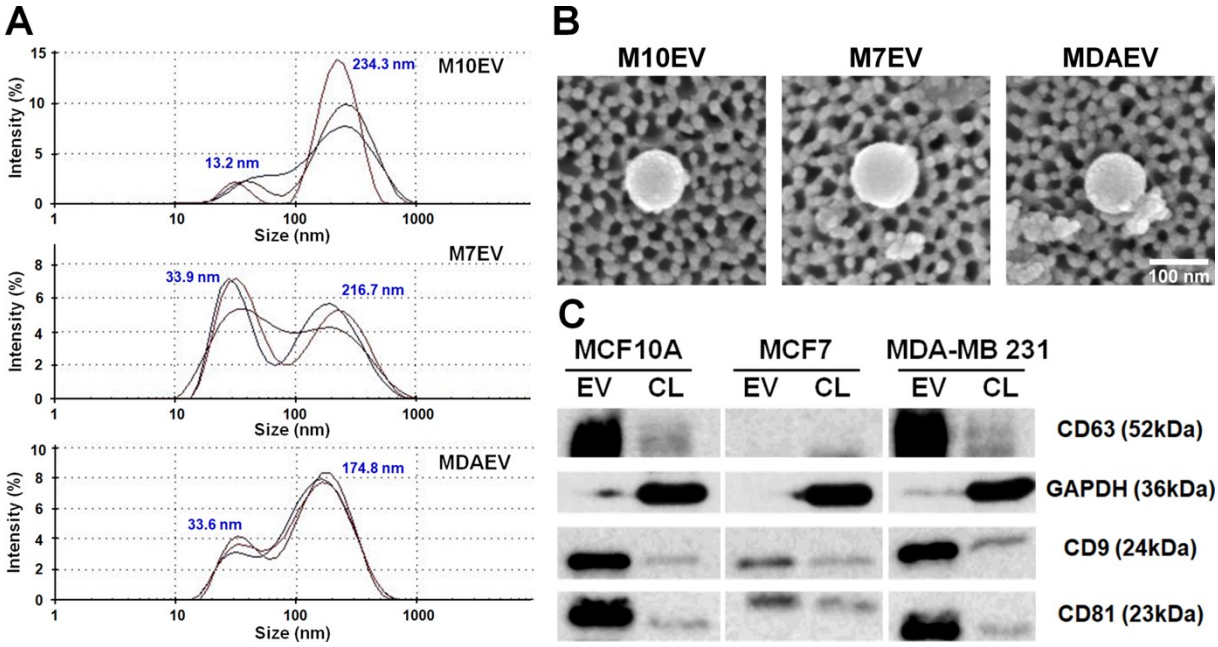

Figure S2. **Characterization and quantification of isolated EVs. (A)** Size distribution of isolated breast epithelial cell-derived EVs using the DLS measurement. **(B)** SEM images of MCF10A, MCF7, and MDA cell-derived EVs (M10AEVs, M7EVs, and MDAEVs, respectively). **(C)** Western blotting for cell-derived EV lysate (EV) and cell lysate (CL) using various markers (CD9, CD63, and CD81 as markers for EVs and GAPDH as a marker for CL)

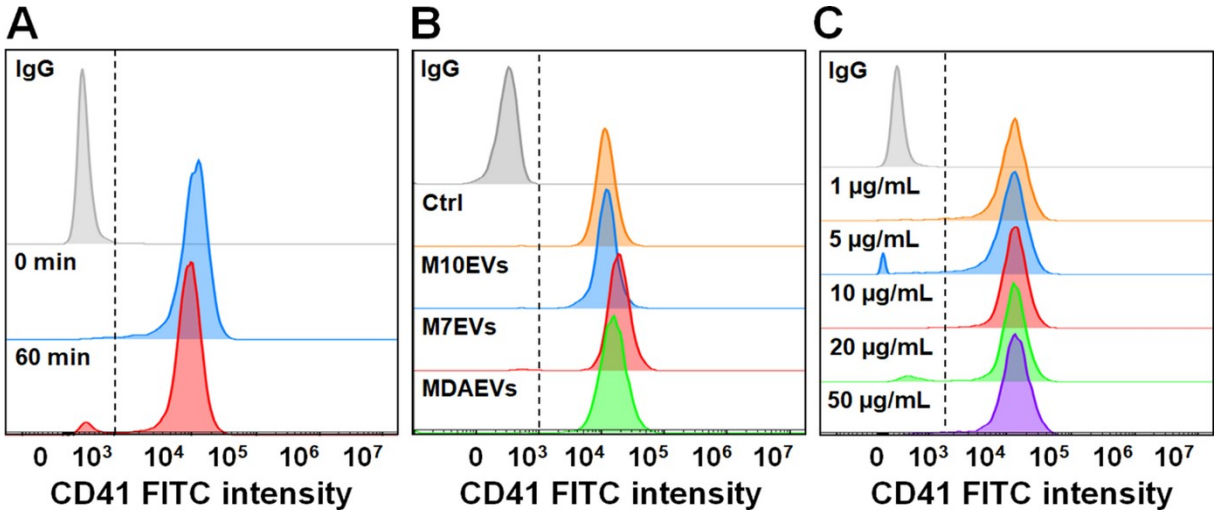

Figure S3. Flow cytometry analysis of CD41 expression as a platelet marker (A) upon exposure to only phosphate-buffered saline (PBS), **(B)** under treatment with 20 µg/mL of various breast epithelial cell-derived EVs for 1h in PBS, and **(C)** various concentrations of MDA-MB 231-derived EVs (MDAEVs) for 1h in PBS. There is no significant difference in the proportion of CD41-positive platelets.

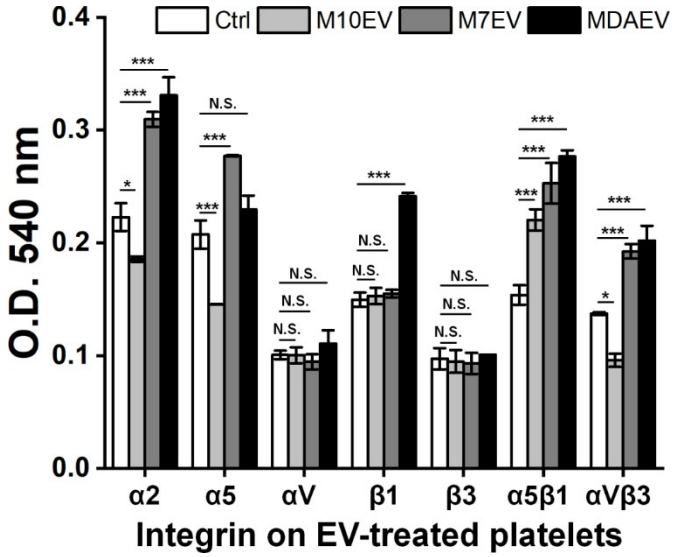

Figure S4. Integrin-specific adhesion array of alpha subunits, beta subunits, and heterodimers on the platelets activated by various epithelial cell-derived EVs. Results are from two separate experiments with pooled platelet samples (n=3). Data indicate the mean ± standard deviation. Two-way analysis of variance with Tukey honestly significant difference post hoc test was used. N.S., non-significant; *, $p < 0.05$; ***, $p < 0.001$.

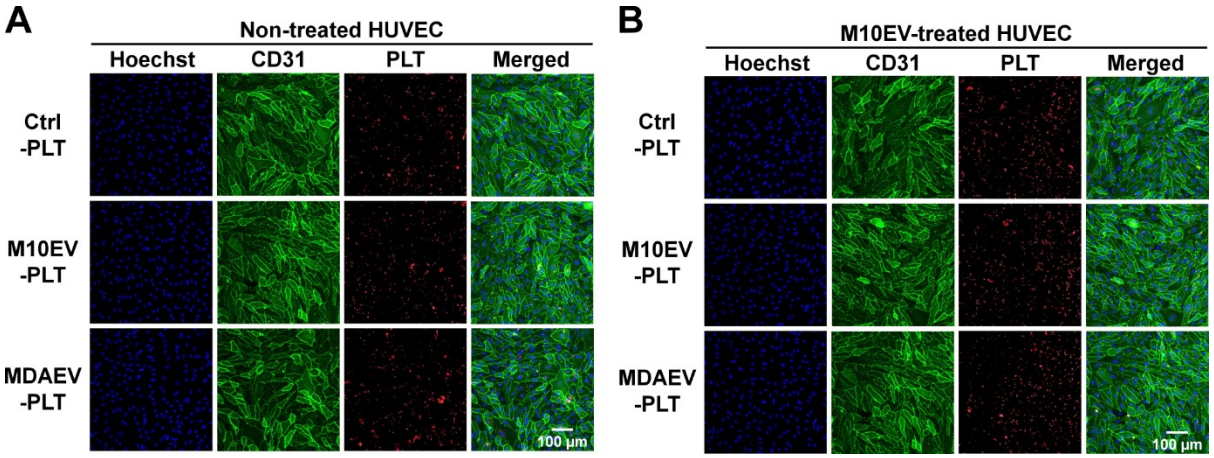

Figure S5. On the normal human vessel, there was no significant change in platelet adhesion under flow, regardless of the type of EVs used for platelet activation. Representative images showing adhesion of platelets (red, CMTPX dye, PLT) activated upon exposure to only PBS (control, Ctrl), by normal breast epithelial cell (MCF10A)-derived EVs (M10EVs), and metastatic MDA-MB 231-derived EVs (MDAEVs) on HUVECs (green, CD-31, also known as platelet endothelial cell adhesion molecule-1 (PECAM-1) pretreated with **(A)** PBS (Non-treated HUVEC) and **(B)** M10EVs (M10EV-treated HUVEC). The nucleus is indicated by Hoechst (blue).

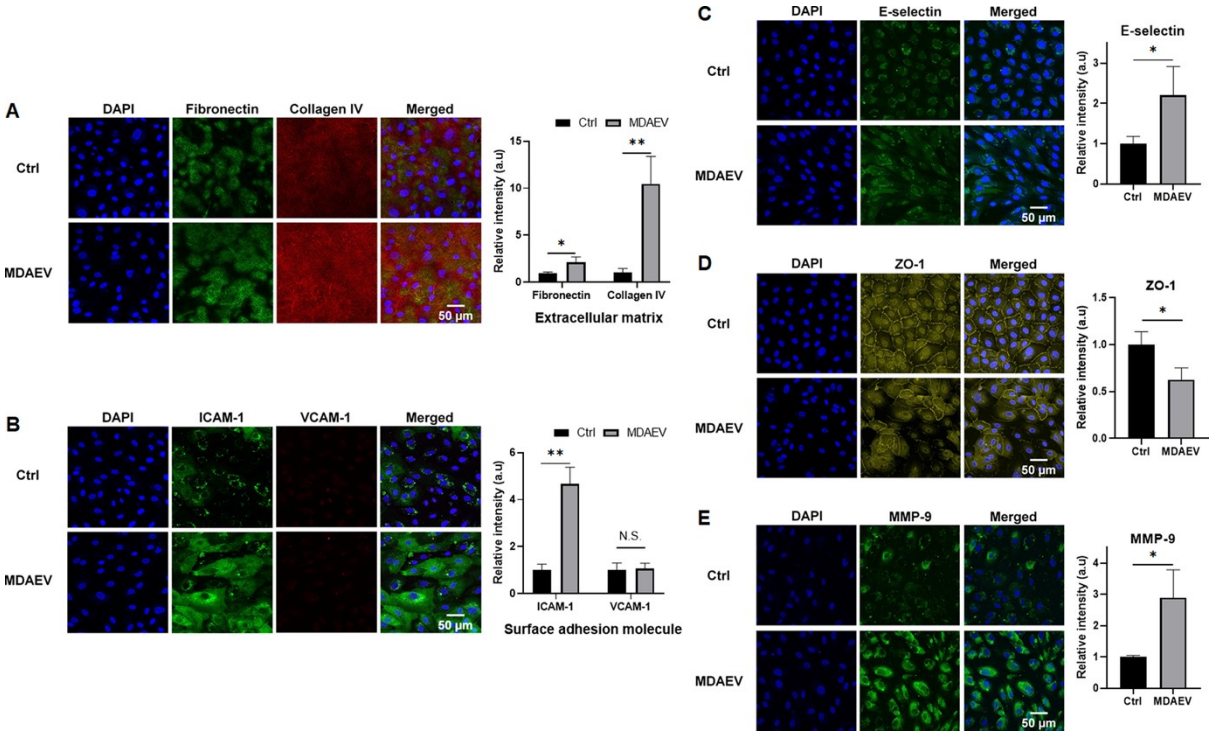

Figure S6. **Representative images and quantification of premetastatic niche formation-related protein expression on vessel chips after treatment with MDAEVs (20 μg/mL) for 24 hours. (A)** Fibronectin and collagen (extracellular matrix marker), **(B)** ICAM-1 and VCAM-1 (surface adhesion molecule marker), **(C)** E-selectin, **(D)** ZO-1 (tight junction marker), **(E)** MMP-9. DAPI is used for staining the nucleus in the endothelial cells in vessel chips. Results are from three separate experiments. Data indicates the mean ± standard deviation. Two-tailed unpaired Student's t-test was used to compare the means of two groups **(C-E)**, and a one-way analysis of variance with Tukey honestly significant difference post hoc test was used **(A and B)**. N.S., non-significant; N.S., non-significant; *, $p < 0.05$; **, $p < 0.01$.

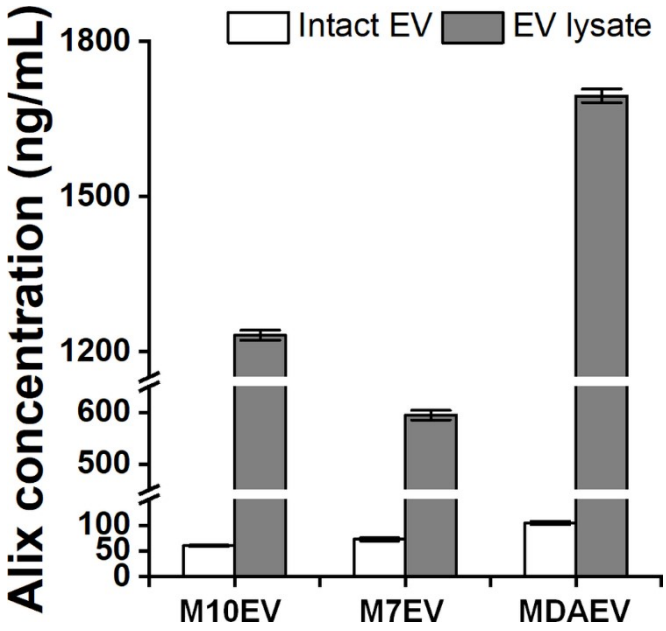

Figure S7. Levels of Alix quantified using ELISA in intact EVs (white bars) and lysates of EVs (grey bars) derived from MCF10A, MCF7, and MDA-MB 231 cells as a negative control for EV surface protein. Graphs indicate the mean ± standard deviation of two measurements of pooled EV samples.

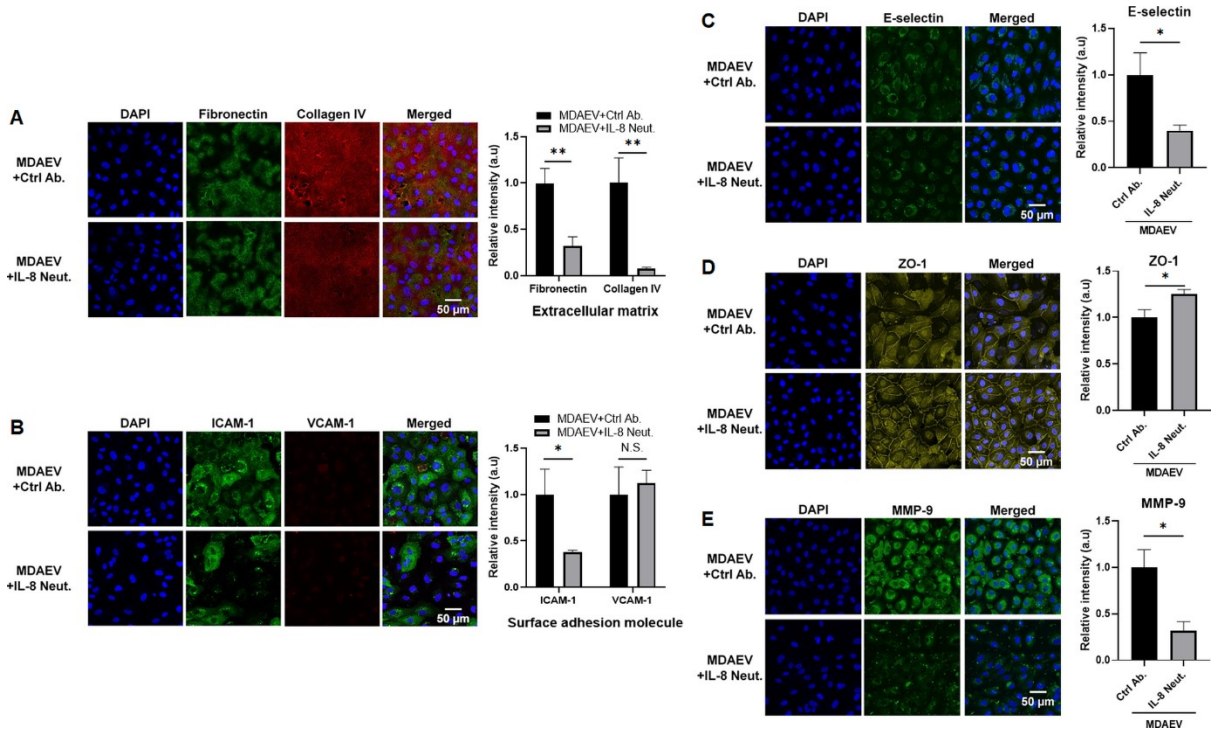

Figure S8. **Representative images and quantification of premetastatic niche formation-related protein expression on vessel chips after treatment with MDAEVs (20 μg/mL) with control antibody or IL-8-neutralizing antibody (0.2 μg/mL) for 24 hours. (A)** Fibronectin and collagen (extracellular matrix marker), **(B)** ICAM-1 and VCAM-1 (surface adhesion molecule marker), **(C)** E-selectin, **(D)** ZO-1 (tight junction marker), **(E)** MMP-9. DAPI is used for staining the nucleus in the endothelial cells in vessel chips. Results are from three separate experiments. Data indicate the mean ± standard deviation. Two-tailed unpaired Student's t-test was used to compare the means of two groups **(C-E)**, and a one-way analysis of variance with Tukey honestly significant difference post hoc test was used **(A and B)**. N.S., non-significant; N.S., non-significant; *, $p < 0.05$; **, $p < 0.01$.

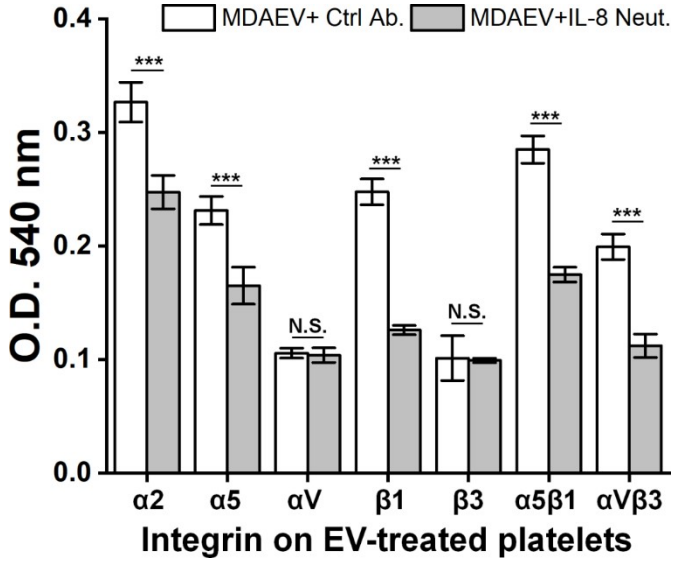

Figure S9. **Integrin-specific adhesion array of alpha subunits, beta subunits, and heterodimers on the platelets activated by pretreatment with control antibody and IL-8-neutralized MDAEVs.** Results are from two separate experiments with pooled platelet samples (n=3). Data indicate the mean ± standard deviation. Two-way analysis of variance with Tukey honestly significant difference post hoc test was used. N.S., non-significant; ***, $p < 0.001$.

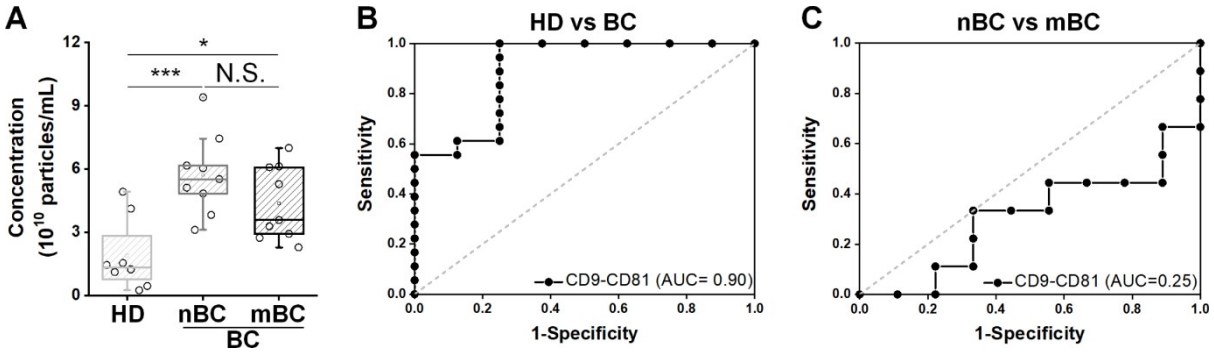

Figure S10. **Prediction of tumor metastasis via particle concentration of EVs in plasma obtained from healthy donors and breast cancer patients in clinical application. (A)** Nanoparticle tracking analysis (NTA) associated with healthy donor (HD)-derived and breast cancer patient (BC)-derived EVs. Plasma samples were collected from eight HDs, nine non-metastatic BCs (nBCs), and nine metastatic BCs (mBCs). The box plot indicates the 75th percentile (top line of the box), median (middle line of the box), 25th percentile (bottom line of the box), as well as 5th and 95th percentiles (whiskers), with raw data presented as scattered dots. One-way analysis of variance with Tukey honestly significant difference post hoc test was used. N.S., non-significant; *, $p < 0.05$; ***, $p < 0.001$. **(B)** Receiver operating characteristic (ROC) curves for distinguishing eight HDs and eighteen BCs using results in particle concentration of EVs obtained from plasma. **(C)** ROC curves for discriminating nine nBCs and nine mBCs using results in particle concentration of EVs obtained from plasma. CI, 95% confidence interval.

Table S1. Comparison of pathologic factors of breast cancer patients according to metastasis status

Variable	[2)]Non-metastatic (n=9)	[3)]Metastatic before blood collection (n=4)	[4)]Metastatic after blood collection (n=5)	[5)]p-value
[1)] Age	49.3±8.9	46±9.3	41.6±7.3	0.17
Subtype				0.624
TNBC	6	2	5	
HR+	3	2	0	
HG				0.35
2	2	2	2	
3	7	2	3	
Site of operation				
breast	9	1	5	
bone metastasis		1		
liver metastasis		2		
Site of metastasis				
lymph node		1	4	
bone		2	5	
brain			3	
liver		4	5	
lung		1	3	
others		3	2	

[1)] Age indicates the age at blood collection from patients.

[2)] Non-metastatic indicates patients who do not have tumor metastasis until follow-up of 3 to 56 months (median 51 months) after operation.

[3)] At blood collection, metastasis had been diagnosed.

[4)] After blood collection, metastasis was diagnosed.

[5)] p-value is calculated between non-metastatic and metastatic.

HG, histologic grade; HR, hormone receptor; TNBC, triple negative breast cancer